Structures and properties of three new homobinuclear nanosized supramolecular copper coordination polymers derived from carboxylate type ligands and benzimidazole

Rasel A. Mukred[a], Samir Osman Mohammed[b,c]

[a]*Department of Biology & Chemistry, College of Education, Al-Baida University, Yemen.*

[b]*Present address: Al-Janad University for Science & Technology, Taiz, Yemen*

[c]*Permanent address: Physics Department, Science Faculty, Ibb University, Yemen*

samir.qa@just.ac

Keywords: *polymer, Molecular Modeling MM2, spectroscopy, thermal analysis, XRD.*

Three new homobinuclear nanosized supramolecular copper coordination polymers are hydrothermally synthesized by self-assembly reaction of L-tyrosine (Tyr), terephthalic acid (H2bdc), pyromellitic acid (H4btec) and benzimidazole (Hbzim) with copper chloride salt to generate with formula $[[Cu_2(tyr)_2(bzim)_2(Cl)2(H_2O)_2]]n$ 1, $[[Cu_2(bdc)_2(bzim)_2(H_2O)_6].3H_2O]n$ 2 and $[Cu_2(H_2btec)(bzim)(H_2O)_6].2H_2O]n$ 3, which have been investigated by elemental analysis, molar conductivity and magnetic measurements, FT-IR and UV-Vis spectroscopy, (TGA/DTA) thermal analysis and X-ray powder diffraction(XRPD) analysis as well as MM2 theoretical calculations. The magnetic moment and electronic spectra of the complexes are certainly indicating the octahedral geometries. Thermal analysis of the complexes confirms the suggested structures and thermal stability. The results of the XRPD analysis and the average nanosized values of the complexes have nanosized supramolecular polymers in the triclinic system. The MM2 theoretical calculations are supported by the proposed structures.

Introduction

Supramolecular chemistry is one of the most promising areas of research in chemistry[1, 2], structural topologies and their various applications as optic, electronic and magnetic devices or microporous materials and antimicrobial activity[1-3]. The design and synthesis of supramolecular coordination polymeric networks have been receiving much attention recently, and the hydrogen bonding and π-πstacking interactions are often employed in their construction, such rational design based on r contacts is a key part of self-assembly supramolecular chemistry[4-6]. One synthetic strategy for the synthesis of the supramolecular coordination polymers is the controlled assembly of donor and acceptor building blocks[7-9]. The Organic aromatic polycarboxylate ligands based on a variety of

View metadata, citation and similar papers at core.ac.uk
brought to you by CORE
provided by French-Ukrainian Journal of Chemistry

carboxylate binding modes have been used to create coordination polymers of different dimensionality in this structurally rich system 1D polymeric chains, 2D polymeric sheets, and 3D polymeric networks with a variety of metal ions reported in the literature[10, 11]. Additionally, the assembly of organic aromatic polycarboxylate and the transition metal ions is highly influenced by the multitopic organic spacer ligands, careful selection of the pH value, solvent system, temperature, counter anions, and metal-to-ligand ratio as well as the coordination nature of the metal ions[12]. All these factors have a significant effect on the formation of desirable frameworks[13, 14]. The benzimidazole as a bidentate ligand is well-known that excellent building blocks in the construction and structural tuning of the resultant MOFs[15, 16]. The L-tyrosine is an amino acid that plays an important role in human life and its pharmacological importance[17, 18]. Supramolecular coordination polymers based on the mixed-ligand systems containing O-donor carboxylates and N-donor heterocyclic ligands have been obtained[19-22]. For example, Wang team have obtained two Co(II) coordination polymers $[[Co(bdc)(bib)(H_2O)]\cdot H_2O]_n$ (1) and $[[Co(bdc)(bibp)]]_n$ (2), where H_2bdc = 1,4-benzenedicarboxylic acid, bib = 1,4-bis(1-imidazolyl)benzene, and bibp = 4,4′-bis(imidazolyl)biphenyl)[23]. H. Lin team, have reported four Cu(II) and Co(II) coordination polymers $[Cu(L)(bdc)(H_2O)]\cdot 3H_2O$ (1), $[Cu(L)(dnba)_2]$ (2), $[Co(L)_2(dnba)_2]$ (3), and $[Co(L)(npiph)(H_2O)]\cdot H_2O$ (4), where H_2bdc =1,4-benzenedicarboxylic acid, Hdnba = 3,5-dinitrobenzoic acid, H_2npiph =5-nitroisophthalic acid and L =N,N-di(3-pyridyl)sebacic diamide[24]. In our study, we focus on assembly reactions of the benzimidazole and copper (II) via hydrothermal synthetic methods with aromatic carboxylate ligands (L-tyr, H_2bdc, H_4btec) to form new homobinuclear nanosized supramolecular copper coordination polymer complexes and described by elemental analysis, molar conductivity, FT-IR and UV-Vis spectra, magnetic susceptibility, TGA/DTA and XRPD analysis as well as MM2 theoretical calculations to elucidate suggested structures as seen here later and influences the aromatic carboxylates, benzimidazole, and copper ion on the structures.

Experimental Section

Chemicals: All the chemicals were obtained from analytical reagent grade (BDH, Aldrich or Fluka).

Preparation of the polymer complexes: The complexes were synthesized by addition of L-tyrosine (0.362 g, 2 mmol / 10 ml) and terephthalic acid (0.332 g, 2 mmol / 10 ml) and pyromellitic acid (0.254 g, 1 mmol / 10 ml) dissolved in a minimum amount of water containing KOH (0.16 mmol / 20 ml) to benzimidazole (0.236 g, 2 mmol / 10 ml) in complexes 1-2 and (0.118 g, 1 mmol / 10 ml) in complex 3, with an aqueous solution of

appropriate $CuCl_2$. $2H_2O$ (0.34 g, 2 mmol / 10 ml) was added with constant stirring and refluxed for 30 min on magnetic stirrer at 25°C (pH= 6.5). The solid product was collected by vacuum filtration, washed several times with cold water, ethanol and anhydrous ether and dried over P_2O_5 in a desiccator vacuum for 24 hours.

Molecular Mechanics (MM2) calculations: The potential energy of all systems in molecular mechanics is calculated using force fields[25]. The optimized geometry, steric energy, and MM2 calculated of the L–tyrosine, terephthalic acid and pyromellitic acid and their complexes were done using the CsChem3D Ultra program package[26].

Physical measurements: Stoichiometric analysis (C, H, N, S) was performed using AnalyischerFunktionstestVario El Fab-Nr.11982027 elemental analyzer. The IR spectra were recorded on a Shimadzu IR-470 spectrophotometer and the electronic spectra were obtained using a Shimadzu UV-2101 PC spectrophotometer. The Thermogravimetric analysis was carried out on a 2000 DuPont thermal analyzer at a heating rate of 10 °C min^{-1}. Magnetic moments were measured at room temperature using a magnetic susceptibility balance of type MSB-Auto. Molar susceptibilities were corrected for diamagnetism of the component atoms by the use of Pascal's constants. The calibrate used to be Hg [Co (SCN) 4]. The X-ray crystallography data were collected using Oxford Gemini Diffractometer at 25°C and Cu-Kα radiation (λ=1.54 Å). The crystal structure was analyzed with the aid of computer software such as Peakfit and Chekcell programs[27, 28].

Results and Discussion

Syntheses and description of the structures: The self-assembly reaction some carboxylates such as tyrosinate and terephthalate and pyromellitate with copper ion and benzimidazole to generate new homobinuclear nanosized supramolecular copper coordination polymer complexes are seen in Figures (1 and 2).

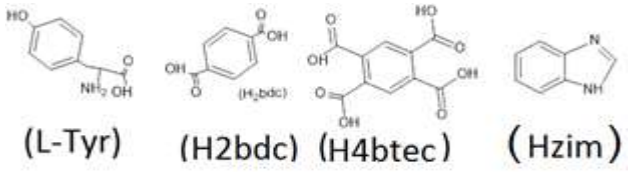

Figure 1. The components of complexes

Based on the physical properties, FT-IR data, UV–Vis data, thermal decomposition data, thermodynamic parameters, and TGA/DTA curves, the three suggested structures of the homobinuclear copper coordination complexes can be represented as follows in Figure (2).

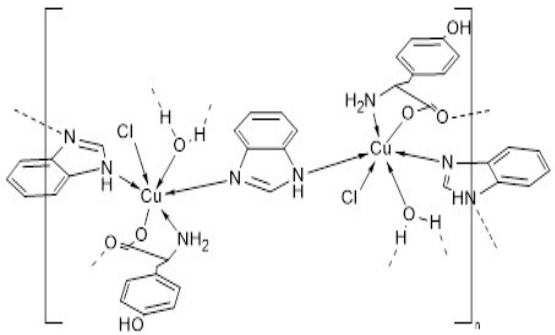

Complex 1

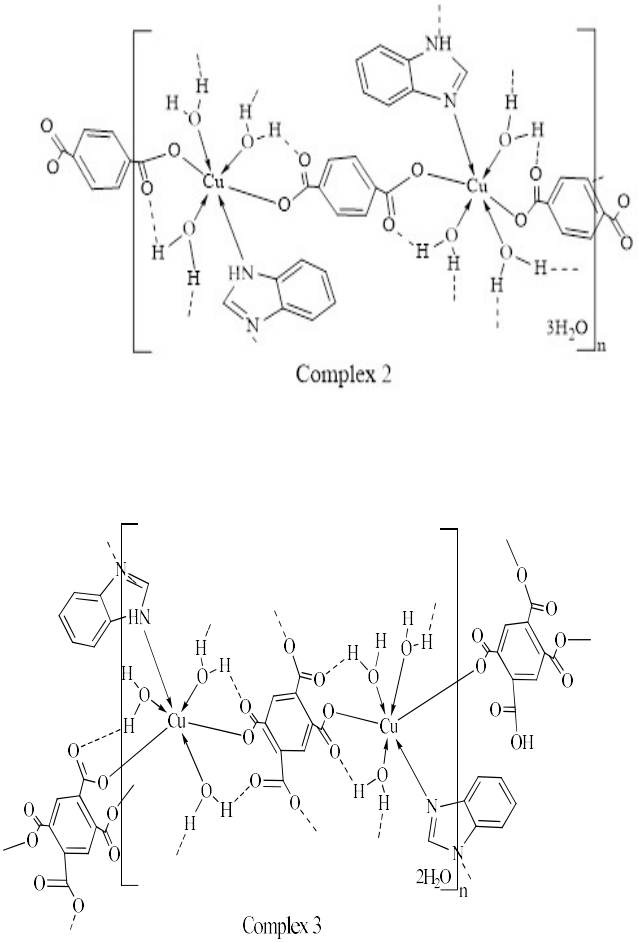

Figure 2. The suggested structures of the prepared complexes.

In the suggested structures are seen in Figure (2), the complexes possess an octahedral geometry. In the structure complex 1, the benzimidazole gives a new type of coordination mode, it acts as bidentate bridge ligand to leading one-dimensional chain with copper (II) tyrosinate complex. In the structure complex 2 and 3, the H_2bdc and H_4btec ligands have an important influence on structures, attributed to differences in substituent groups positions of carboxylic groups and numbers of the carboxylic groups and positions copper ions. The suggested structures of the complexes exhibit may be supramolecular coordination polymer structures through hydrogen bonding interactions involving the constituent materials which enhance the stability of these complexes[29, 30]. The hydrogen bond affording the possibility of participation in intermolecular and/or intramolecular hydrogen bonding interactions. The hydrogen-bonding interactions, the first type is O-H..O hydrogen bonds in the presence of many uncoordinated water molecules are connected between the hydrogen atoms and carboxylate oxygen atoms in intramolecular, the second type is O...H_O hydrogen bonds exist of the coordinated water molecules are connected between the hydrogen atoms and carboxylate oxygen atoms intramolecular, the third type is O...H_O hydrogen bonds, inter-sheet maybe contacted are strengthened by π-π*interactions, and three hydrogen bond types are importing factor in the supramolecular assembly and stability of these complexes and also maybe act to hold the chains together within the 3D architecture[31-33].

Conductivity measurement: The coordination polymer complexes showed values at 13.78, 15.69 and 36.80 $ohm^{-1}cm^2$ mol^{-1} listed in Table 1, indicating non-electrolyte in DMSO[34]. These results are common with supramolecular polymers and coordination polymers, these complexes are insoluble in common solvents such as methanol, water, and acetonitrile but soluble in N, N-dimethylformamide (DMF) and dimethyl sulfoxide (DMSO).

Table 1. Physical properties of coordination polymer complexes

Complexes	Color	ΛM ohm^{-1} cm2mol^{-1}	M.P (ºC) (Decomp.)	% Analysis, found (calced)			
				C%	H%	N%	μeff (B.M)
1	Dark -blue	13.78	> 320	47.54 (46.15)	5.16 (4.37)	10.24 (10.95)	1.72
2	Dark - blue	15.69	> 320	45.45 (44.82)	5.81 (6.12)	7.14 (6.33)	1.67
3	Dark -blue	36.80	>360	44.65 (43.67)	4.78 (4.28)	9.29 (8.49)	1.87

IR spectra and mode of bonding:

From the FT-IR spectra, there are some bands appeared in the polymer complexes spectra which are attributed to M-O and M-N, these two bands confirm the complexes formation. The ν(C=N) band of the benzimidazole occurs at 1470, 1480 and 1490 cm^{-1}[35]. In the free L-tyr ligand the bands of ν_{as}(COO) and ν_{s}(COO) located about 1612 and 1416 cm^{-1}, respectively, a notable shift to a lower frequency at 1605 and 1390 cm^{-1}, due to the ν_{as}(COO) and ν_{s}(COO), respectively, in the complex 1 as in Figure(3), the separation (Δν=215 cm^{-1}), indicates that the tyrosinate behaved as bidentate fashion[36].

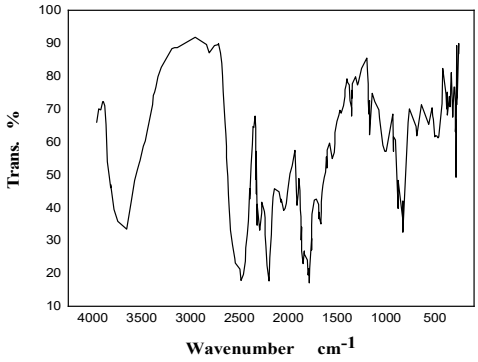

Figure 3. FT-IR Spectrum of the copper polymer complex 1

In the FT-IR spectrum comparison of the free H2bdc ligand with complex 2, as in Figure(4). In the ligand, the band exhibit at 1680 cm^{-1} is ascribed to νas(COO) and 1420 cm^{-1} is attributed to the νs(COO), whereas these bands shifted to a lower frequency in the complex 2 at 1575 cm^{-1} and 1380 cm^{-1}, respectively. In the complex 2, as in Figure(4), the separation Δν=195 cm^{-1} typical indicates a monodentate fashion.[37, 38]

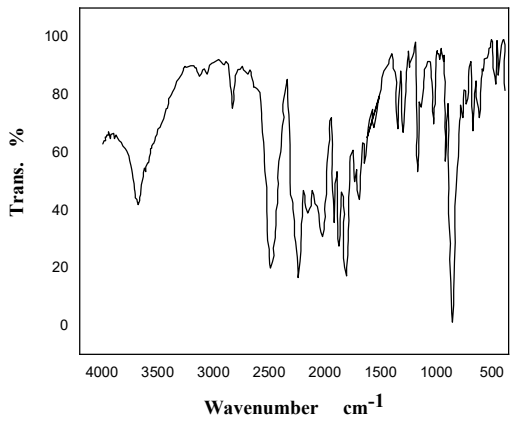

Figure 4. FT-IR Spectrum of the copper polymer complex 2

In the FT-IR spectrum comparison of the free H_4btec ligand with complex 3, as in Figure (5). The absence of any strong bands around 1720 cm^{-1} indicates that all carboxylic groups are deprotonated. In the ligand, the bands of ν_{as}(COO) and ν_s(COO) exhibits at 1500 and 1380 cm^{-1}, respectively, these bands shifted to a higher frequency in the complex-3 at 1580 cm^{-1} and 1390 cm^{-1}. In the complex 3, as in Figure(5), the separation ($\Delta\nu$ = 190 cm^{-1}) value proved that the carboxylate group is coordinated to the copper ion in a monodentate fashion.[39-41]

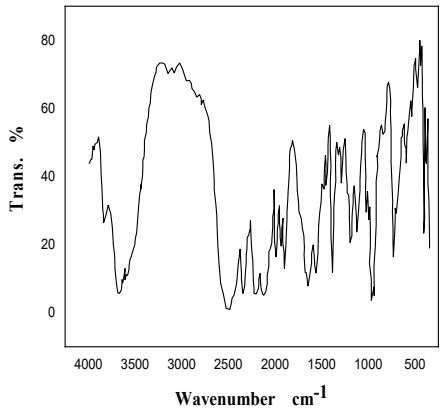

Figure 5. FT-IR Spectrum of the copper polymer complex 3

The ν(O–H) stretching vibration of coordinated water for the complexes 2 and 3 are located at 2900 and 2900 cm^{-1}[42], whereas the ν(O–H) of the uncoordinated water of the complexes are assigned to the bands in the 3600, 3450 and 3400 cm^{-1}[43]. The most important bands which appeared in the 550, 520 and 540 due to ν(M–O) and 450, 480 and 450 cm^{-1} due to ν(M–N), these bands confirm the complexes formation and represent further evidence for the coordination of the ligands through both nitrogen and oxygen atoms.

UV-Vis spectra and magnetic susceptibility measurement: The FT-IR spectra were recorded on a Shimadzu IR-470 The electronic spectra of the coordination polymer complexes were recorded in DMSO and in Figure (6). The third band for complexes appearing at 18466, 18726 and 18832 cm^{-1}, respectively, which may be assigned to the $^2Eg \rightarrow {}^2T_2g$ transition indicating octahedral geometry around copper ion,[44] and showed magnetic properties with μ_{eff} values of 1.72, 1.67 and 1.87 B.M, respectively, listed in Table 1. The low values due to weak antiferromagnetic interaction because of the long distance between the two magnetic copper centers with homobinuclear complexes. The suggested structures of these complexes are shown in Figure (2).

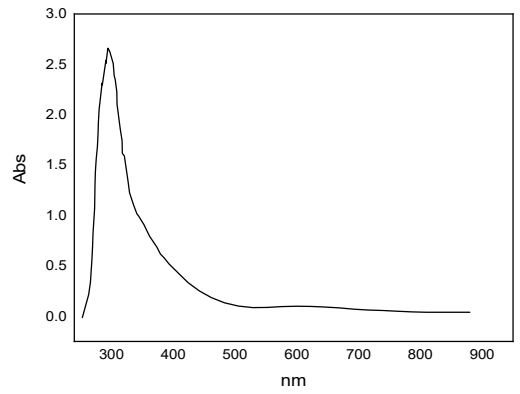

Complex1

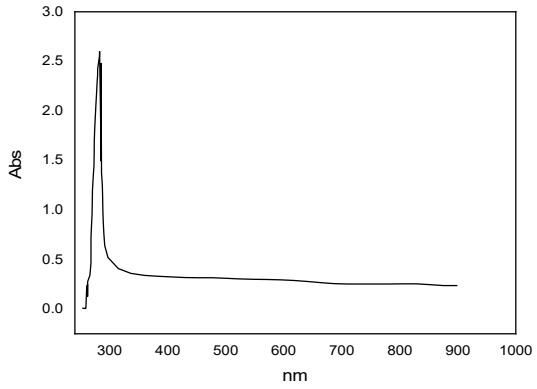

Complex2

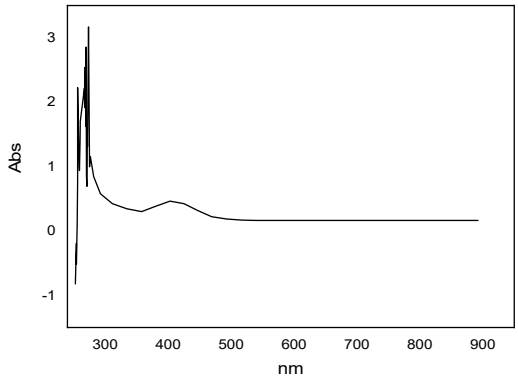

Complex3

Figure 6. UV-Vis spectrum of the copper polymer complexes

Thermogravimetric analysis: The thermal stability of the coordination polymer complexes was investigated by TGA/DTA in the air flow in the Tables 2-4 and the structures are observed in the TGA/DTA spectra in Figures (7-9)[45].

***Thermal decomposition*:** The thermal decomposition of the polymer complex 1 $[[Cu_2(tyr)_2(bzim)_2(Cl)_2(H_2O)_2]]_n$, from 31-482ºC listed in Table 2 and TGA/DTA spectra is shown in Figure (7), it decomposes in three steps, the initial weight loss occurring in the range 31–209ºC, with the release of two coordinate water molecules (calc. 4.32 %, found 3.62 %) and it is connected with an activation energy of 36.49 kJ/mol. The DTG curve exhibits a peak at 50ºC and an exothermic DTA curve gives a peak at 52ºC. The second step of decomposition in the range 210-283ºC (calc. 14.18 %, found 13.85 %) corresponds to the loss of the one bzim ligand and activation energy of 114.73 kJ/mol. The DTG curve exhibits midpoint at 249ºC, which is associated with an exothermic DTA curve that gives a peak at 253ºC. The third is composed of three overlapping steps of mass loss in the range 284–482ºC (calc. 50.13 %, found 51.84 %) corresponds to the loss of the Tyr and bzim ligands from the anhydrous complex, a three DTG curve exhibits peaks at 289, 357 and 403ºC and the exothermic DTA curve gives three peaks at 290, 358 and 405ºC are observed. The corresponding activation energy amounts to 192.21KJ/mol. After this, the complex decomposes continuously till 482 ºC, the decomposition mechanisms proposed for the copper complex are summarized by equation 1:

$$[Cu_2(tyr)_2(bzim)_2(Cl)_2(H_2O)_2]_n \frac{31-209^oC}{-2H_2O} \rightarrow [Cu_2(tyr)_2(bzim)_2(Cl)_2] \frac{210-283^oC}{-bzim} \rightarrow$$

$$[Cu_2(tyr)_2(bzim)(Cl)_2] \frac{284-482^oC}{-bzim+tyr} \rightarrow [Cu_2(tyr)(Cl)_2] \frac{After}{741^oC}$$

$$\rightarrow Compex\ decomposes\ continuously \quad (1)$$

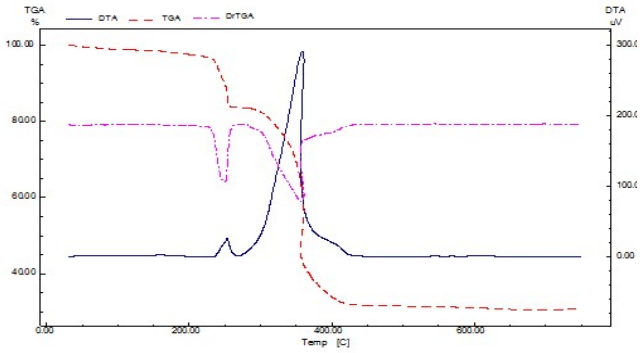

Figure 7. TGA – DTA - DrTGA curves of complex 1

Table 2. Thermal decomposition data of complex 1

Step	Temp. range(°C)	Weight loss (%)		Assignment	DTG (°C)	DTA (°C)
		Found	Calc			
1st	31–209	3.62- 4.32		Loss of two coordinated water molecules	50	52
2nd	210-283	14.85- 14.18		Loss of the one bzim ligand	249	253
3rd	284–482	51.84 -50.13		Loss of the tyr and bzim ligands	289, 357, 403	290, 358, 405

The thermal decomposition of the polymer complex 2 $[[Cu_2(bdc)_2(bzim)_2(H_2O)_6].3H_2O]_n$, from 31-748°C listed in the Table 3 and TGA/DTA spectra, is shown in Figure (8), the first is composed of two overlapping steps of mass loss occurring in the range 31-171°C, (calc. 6.29 %, found 5.87 %)with the elimination of three uncoordinated water molecules and the corresponding activation energy of 179.06KJ/mol, the DTG curve exhibits two peaks at 79 and 113°C and an endothermic DTA curve gives two peaks at 82 and 126°C. The second step is composed of three overlapping steps of mass loss in the range 172-308°C and (calc. 12.59 %, found 12.18 %) corresponds to the loss of the six-coordinate water molecules with an activation energy of 104.23 kJ/mol. A DTG curve exhibits three peaks at 135, 190 and 242°C and the exothermic DTA curve gives two peaks at 136 and 289°C and DTA curve gives peak an endothermic 191°C and exothermic, were observed. The third step is decomposed in the range 309-421°C (Calc. 33.14 %, found 32.77 %) corresponds to the loss of the bdc and bzim ligands, the computed activation energy amounts

to 160.51 kJ/mol. A DTG curve exhibits a peak at 385°C and the exothermic DTA curve gives a peak at 392°C, were observed. The fourth step is composed of two overlapping steps of mass loss in the range 422–748°C (calc. 33.14 %, found 32.54 %) indicates decomposition of the bdc and bzim ligands and activation energy amounts to 206.99 kJ/mol. The DTG curve exhibits two peaks at 476 and 529°C and exothermic two DTA curves give peaks at 475 and 535°C. The final product indicates that the residue is 2CuO (Calc. 18.54 %, found 16.74 %), the decomposition mechanisms proposed for copper complex 2 are summarized by equation 2:

$$[Cu_2(bdc)_2(bzim)_2(Cl)_2(H_2O)_6 \cdot 3H_2O]_n 2 \frac{31-308^oC}{-9H_2\,O} \rightarrow [Cu_2(bdc)_2(bzim)_2] \frac{309-421^oC}{-bdc+bzim}$$

$$\rightarrow [Cu_2(bdc)(bzim)] \frac{422-748^oC}{-bdc+bzim} \rightarrow 2CuO + Decomposition\ products \quad (2)$$

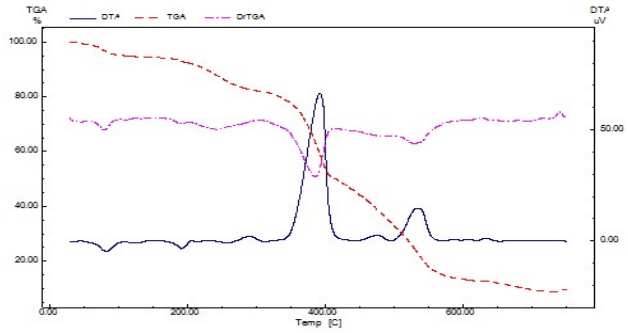

Figure 8. TGA-DTA-DrTGA curves of the polymer complex 2

Table 3. Thermal decomposition data of complex 2

Step	Temp. Range (°C)	Weight loss (%)		Assignment	DTG (°C)	DTA (°C)
		Found	Calc			
1st	31–171	5.87	-6.47	Loss of three uncoordinated water molecules	79, 113	82, 126
2nd	172-308	12.18	- 12.59	The loss of six coordinate water molecules	135, 190, 242	136, 190, 289
3rd	309-421	32.77	- 33.14	Loss of the bdc and bzim ligands	385	392
4th	422-748	32.54	- 33.14	Loss of the bdc and bzim ligands	476, 529	475, 535

The thermal decomposition of the polymer complex 3 $[Cu_2(H_2btec)(bzim)(H_2O)_6].2H_2O]n$, from 28-747 °C listed in Table 4 and TGA/DTA spectra is shown in Figure (9), its decompose in four steps, the initial weight loss release of two uncoordinated water molecules (calc. 5.62 %,

found 5.56 %) in the range 28–80 ºC, this step has an activation energy value of 58.63 kJ/mol. The DTG curve exhibits a peak at 54 ºC and the endothermic DTA curve gives a peak at 66 ºC. The second step is composed of three overlapping steps of mass loss (calc. 16.36 %, found 17.74 %), corresponds to the loss of the six coordinated water molecules in the range 81–257 ºC, the DTG curve exhibits three peaks at 98, 132 and 232ºC and an endothermic DTA curve gives three peaks at 102, 136 and 225ºC, are observed. It is connected with an activation energy of 184.54 kJ/mol. The third step of decomposition in the range 258–456ºC (calc. 20.12 %, found 19.55 %), corresponds to the loss of the one bzim ligand, a DTG curve exhibits a peak at 332ºC and the exothermic DTA curve gives a peak at 297ºC, are observed. The corresponding activation energy amounts to 113.81 KJ/mol. The fourth step is composed of three overlapping steps of mass loss (calc. 39.31 %, found 40.19 %) corresponds to the loss of the one btec ligand in the range 457–747 ◦C, a DTG curve exhibits three peaks at 550, 652 and 685ºC and the endothermic DTA curve give peaks at 557 and 690ºC, exothermic DTA peak 660ºC, are observed. The corresponding activation energy amounts to 322.43KJ/mol. The final product indicates that the residue is 2CuO (calc. 24.68 %, found 22.5 %), the decomposition mechanisms proposed for copper complex 3 are summarized by equation 3:

$$[Cu_2(btec)(bzim)(H_2O)_6 \cdot 2H_2O]_n 3 \xrightarrow{28-257^oC} \xrightarrow[-8H_2\,O]{} [Cu_2(btec)(bzim)] \xrightarrow[-bzim]{258-456^oC} \rightarrow$$

$$[Cu_2(btec)] \xrightarrow[-btec]{457-747^oC} \rightarrow 2CuO + Decomposition\ products \quad (3)$$

Table 4. Thermal decomposition data of complex 3

Step	Temp. Range (ºC)	Weight loss (%)		Assignment	DTG (ºC)	DTA (ºC)
		Found	Calc			
1st	28-80	5.56 – 5.62		Loss of two uncoordinated water molecules	54	66
2nd	81–257	17.74 – 16.36		Loss of six coordinate water molecules	98, 132, 232	102, 136, 225
3rd	258–456	19.55 – 20.12		Loss of the one bzim ligand	332	297
4th	457–747	40.19 – 39.31		Loss of the btec ligand	550, 652, 685	557, 660, 690

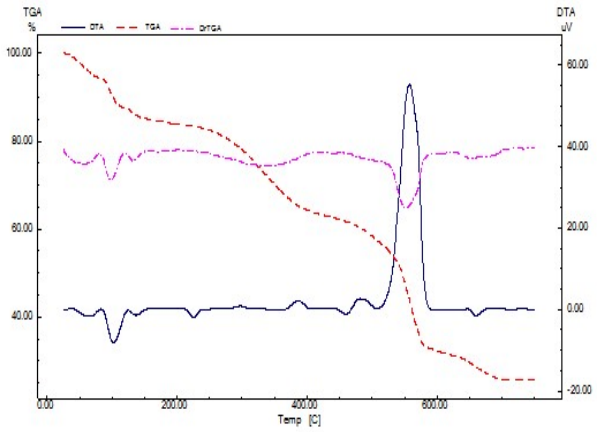

Figure 9. TGA-DTA-DrTGA curves of the polymer complex-3

Kinetic analysis: The order of the reaction (n), activation energy (E) and the pre-exponential factor (Z) of the different stages of thermal decomposition reactions for the first dehydration step have been evaluated from the TGA curve by using Coats–Redfern equations 4 and 5 and Horowitz-Metzger equations 6 and 7. [46-48] The plot of

$$ln\left[\frac{1-(1-\alpha)^{1-n}}{(1-n)}\right]=\frac{M}{T}+B \qquad for \quad n\neq 1 \quad (4)$$

or

$$ln\left[-ln\frac{(1-\alpha)}{T^2}\right]=\frac{M}{T}+B \qquad for \quad n\neq 1 \quad (5)$$

where α is the fraction of material decomposed, n is the order of the decomposition reaction and M=E/R and B=ZR/ΦE; E, R, Z and Φ are the activation energy, gas constant, pre-exponential factor and heating rate, respectively. The plot of

$$ln\left[\frac{1-(1-\alpha)^{1-n}}{(1-n)}\right]=ln\frac{ZRT_s^2}{\emptyset E}-\frac{E}{RT_s}+\frac{E\theta}{RT_s^2} \qquad for \quad n\neq 1 \quad (6)$$

$$ln\frac{E}{RT_s}=ln\frac{Z}{\emptyset}-\frac{E}{RT} \qquad for \quad n\neq 1 \quad (7)$$

where θ=T-T_s, T_s is the temperature at the peak of DTG. The change in the activation enthalpy ΔH, activation entropy ΔS and the free energy of activation ΔG were calculated and listed in Tables 5 and 6. The negative value of entropy also indicates that the activated complexes have a more ordered and more rigid structure than the reactants or intermediates.

Table 5. Kinetic and thermodynamic parameters of the complexes in dynamic air flow (Coats–Redfern) Order (n), Z (s^{-1}), E (kJ mol^{-1}), Δ H (kJ mol^{-1}), ΔS (JK^{-1} mol^{-1}), ΔG (kJ mol^{-1})

Comp.	Step	*n*	*r*	*ΔE*	*Z*	*ΔH*	*-ΔS*	*ΔG*
1	1st	1.00	-0.99944	36.49	3.04×10^{5}	32.74	0.15172	101.34
	2nd	0.00	-0.99941	114.73	2.44×10^{-1}	110.39	0.2695	251.21
	3rd	0.00	-0.99983	192.21	2.46×10^{-5}	186.96	0.34766	406.17
2	1st	2.00	-0.99998	179.06	7.12×10^{-17}	176.35	0.563075	359.73
	2nd	2.00	-0.98250	104.23	3.38×10^{-2}	100.38	0.285043	232.35
	3rd	2.00	-0.99935	160.51	2.23×10^{-6}	156.23	0.36595	344.68
	4th	2.00	-0.99749	206.99	4.25×10^{-6}	201.52	0.36263	440.14
3	1st	2.00	-0.97756	58.63	6.43283	55.91	0.23851	133.84
	2nd	2.00	-0.9802	184.54	3.60×10^{16}	181.46	0.55068	385.80
	3rd	2.00	-0.97752	113.81	9.19404	108.77	0.24068	254.70
	4th	2.00	-0.99112	322.43	1.07×10^{-9}	315.59	0.43338	672.27

Table 6. Kinetic and thermodynamic parameters of the complexes in dynamic air atmosphere (Horowitz-Metzger) Order (n), Z (s^{-1}), E (kJ mol^{-1}), Δ H (kJ mol^{-1}), ΔS (JK^{-1} mol^{-1}), ΔG (kJ mol^{-1})

Comp.	Step	*n*	*r*	*ΔE*	*Z*	*ΔH*	*-ΔS*	*ΔG*
1	1st	1.00	0.99991	43.21	4.42×10^{4}	39.45	0.15943	111.54
	2nd	0.00	-0.99952	123.52	6.36×10^{11}	119.18	0.02360	131.49
	3rd	0.00	-0.99546	202.39	1.6×10^{16}	197.15	0.05908	234.41
2	1st	2.00	0.999998	184.69	4.57×10^{27}	181.76	0.28320	281.64
	2nd	2.00	0.983927	111.84	3.6×10^{12}	107.99	0.00820	111.79
	3rd	2.00	0.99925	169.05	1.29×10^{17}	164.77	0.07812	205.01
	4th	2.00	0.99749	217.89	1.12×10^{17}	212.42	0.07492	261.72
3	1st	0.00	0.981663	64.23	6.66×10^{9}	61.52	0.0576	80.34
	2nd	2.00	0.98114	190.51	9.74×10^{26}	187.42	0.26993	287.58
	3rd	2.00	0.99667	126.08	2.55×10^{10}	121.04	0.05156	152.30
	4th	2.00	0.99172	336.12	1.08×10^{21}	329.28	0.14931	452.17

The large negative entropy of activation and high free energy of activation denote a slow reaction and consequently stable complexes[49]. The high values of the activation energies, reflect the thermal stability of the complexes[50, 51]. The values of ΔG increase for the subsequent decomposition steps reflects that the rate of removal of the subsequent ligand will be lower than that of the preceding ligand due to the structural rigidity of the remaining copper polymer complex after the expulsion of one ligand and more ligand removal will require more energy for its rearrangement before undergoing any compositional change[44, 52, 53]. Based on the information gained from the above results, the suggested structures of these complexes can be seen in Figure (2).

X-ray powder diffraction: The X-ray powder diffraction patterns of the three copper coordination polymer complexes are shown in Figure (10). There are many computer codes that have been used to analyze the X-ray line profile. We have used the residual-peak fitting (PeakFit) software. This program helps to detect, separate, quantify hidden peaks that standard instrumentation misses and background correction. PeakFit also includes different nonlinear spectral application line shapes. There are three AutoFit peaks options offered by PeakFit software[27]. We have selected one of these options. In this option, the hidden peaks are detected by the "sharpening" achieved by deconvolving a Gaussian instrument response to the raw data. The baseline is also fitted with a Gaussian deconvolution procedure. The fitting procedure also ensures a good convergence factor.

We have used the standard cell parameters for the three complexes[54] as starting values for “CHEKCELL” program to identify the Bragg reflections. CHEKCELL program is a powder Indexing software. The crystal lattice parameters were computed with the aid of the computer program Chekcell[28].

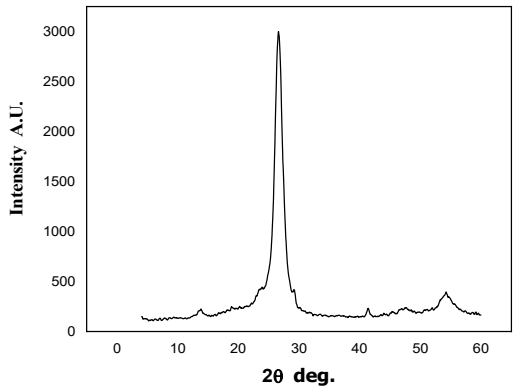

Complex1

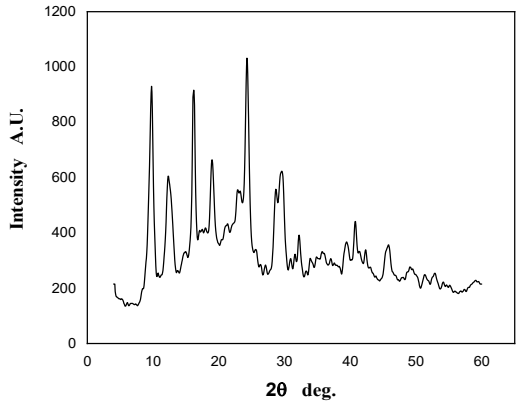

Complex2

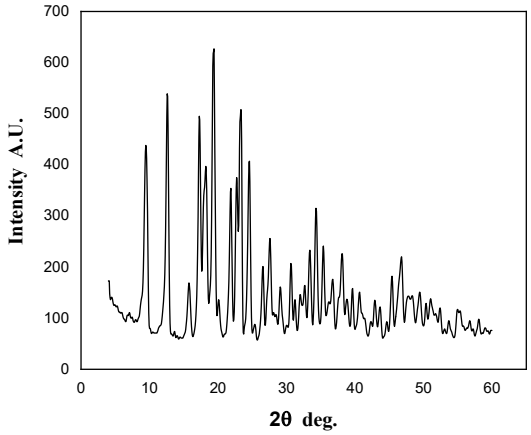

Complex3

Figure 10. XRD pattern of complexes

The crystal data of these complexes are observed and fitted well with the triclinic crystal system. The unit cell parameters of the complexes are given in Table 7.

Table 7. Unit cell parameters of the copper polymer complexes

Parameters	Comp.1	Comp.2	Comp.3
Crystal system	Triclinic		
Space group	p1		
a (Å)	10.010	9.432	9.453
b (Å)	14.971	12.726	12.709
c (Å)	21.875	17.575	17.578
α (°)	90.58	90.18	90.17
β (°)	109.12	99.93	100.03
γ (°)	90.05	90.17	90.26
Volume of unit cell $(Å)^3$	3097.14	2077.87	2079.82

***Nanosized analysis*:** From the indexed data, the unit cell parameters which calculated and recorded in Table (7). Furthermore, using the diffraction data, the mean crystallite sizes of the complexes, *D*, were determined according to the Scherer equation:($D = 0.9\lambda/(\beta\cos\theta)$, where λ is X-ray wavelength (1.54056 Å), θ is Bragg diffraction angle, and β is the full width at half maximum of the diffraction peak[55]. The average crystallite sizes of the three complexes were found to be 72.27 nm, 111.54 nm and 194.39 nm. The values indicate that complexes 2 and 3 are more crystalline than that complex 1. The Figure (10) show the crystalline nature of the three copper polymer complexes and the peak sharpness in the XRD patterns indicates the existence of the nanosized supramolecular polymers.

Molecular modeling studies: In order to get finer structural details of polymer complexes, we have optimized and MM2 calculated the

molecular structure of complexes[25]. Therefore, we could obtain the optimized geometry for each complex by competing for the minimum steric energy and the theoretical physical parameters, such as bond lengths and bond angles using the Chem3D Ultra program package. The optimized structures of these complexes in Figure (11) were some selected calculated parameters in the coordination sphere in Tables 8-10. In these complexes, coordination by chelation involving the various modes of oxygen, nitrogen and chloride are possible. The results reveal the presence of an octahedral geometry in the complexes. The reveals minimum steric energies values studied of four ligands and their complexes (7.75 kcal/mol for L-tyrosine, 20.63 kcal/mol for terephthalic acid, 80.9592 kcal/mol for pyromellitic acid and 9.62 kcal/mol for benzimidazole, 199.32 kcal/mol for complex 1, 223.83 kcal/mol for complex 2 and 230.32 kcal/mol for complex 3). MM2 calculated of complexes is in good agreement with proposed compositions of the complexes based on elemental analysis.

Complex1

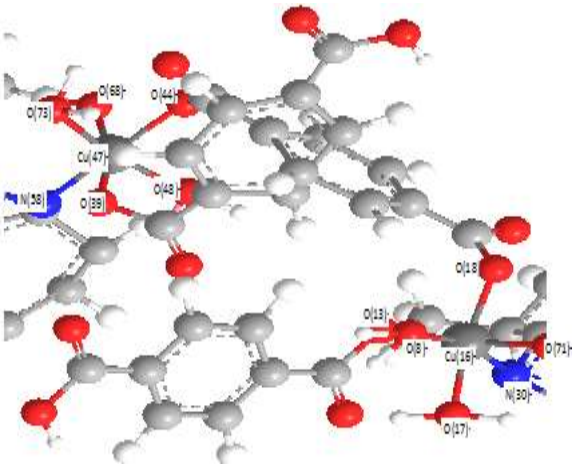

Complex2

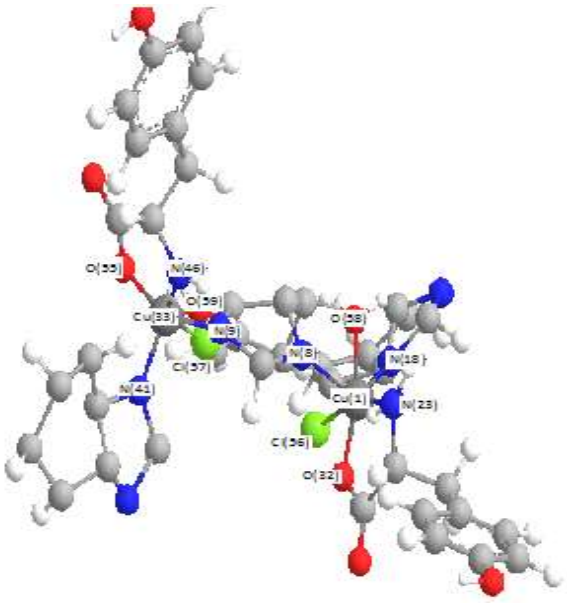

Complex 3

Figure 11. Optimized structure of complexes

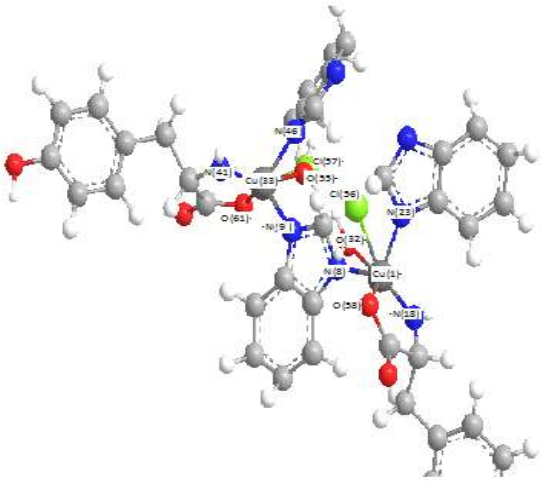

Conclusions

Based on the above analysis and spectroscopic evidence, magnetic data and MM2 theoretical studies, we hydrothermally synthesized of the new nanosized homobinuclear coordination polymer complexes and have octahedral geometry. From the FT-IR spectra of the complexes are completely deprotonated in these ligands proves very clearly that the complexes

are supramolecular coordination polymers. The suggested structures of complexes reveal that the carboxylates, benzimidazole, and copper ion have an influence on the structures. The FT-IR spectra of the complexes are completely deprotonated in these ligands proves very clearly that the complexes are supramolecular coordination polymers. Thermogravimetric analysis of the complexes showed thermal stability and suggested structures. In addition, the first step towards H_2O release is important in the TGA/DTA thermal analysis of the investigated of these complexes and it is usually regarded as participating in extensive structure hydrogen bonding because it is an important factor in the stabilization of lattice and supramolecular assemblies. The XRD patterns and average particle size values indicated the crystalline nature of the complexes and confirm the existence of the nanosized supramolecular polymers. The MM2 calculations were performed to obtain the theoretical information on the structures which was confirmed by the experimental results.

References

[1] Ariga K, Kunitake T. Supramolecular chemistry-fundamentals and applications: advanced textbook: Springer Science & Business Media; 2006.

[2] Bosman AW, Sijbesma RP, Meijer E. Supramolecular polymers at work. Mater Today. 2004;7(4):34-9.

[3] Patra D, Ramesh M, Sahu D, Padhy H, Chu CW, Wei KH, et al. Synthesis and applications of a novel supramolecular polymer network with multiple H-bonded melamine pendants and uracil crosslinkers. J Polym Sci, Part A: Polym Chem. 2012;50(5):967-75.

[4] Burattini S, Greenland BW, Merino DH, Weng W, Seppala J, Colquhoun HM, et al. A healable supramolecular polymer blend based on aromatic π− π stacking and hydrogen-bonding interactions. J Am Chem Soc. 2010;132(34):12051-8.

[5] Aida T, Meijer E, Stupp SI. Functional supramolecular polymers. Science. 2012;335(6070):813-7.

[6] Obert E, Bellot M, Bouteiller L, Andrioletti F, Lehen-Ferrenbach C, Boué F. Both water-and organo-soluble supramolecular polymer stabilized by hydrogen-bonding and hydrophobic interactions. J Am Chem Soc. 2007;129(50):15601-5.

[7] Das A, Ghosh S. Supramolecular assemblies by charge-transfer interactions between donor and acceptor chromophores. Angew Chem Int Ed. 2014;53(8):2038-54.

[8] Wang Y, Xu H, Zhang X. Tuning the amphiphilicity of building blocks: controlled self-assembly and disassembly for functional supramolecular materials. Adv Mater. 2009;21(28):2849-64.

[9] Evans NH, Beer PD. Advances in anion supramolecular chemistry: from recognition to chemical applications. Angew Chem Int Ed. 2014;53(44):11716-54.

[10] Ghosh SK, Bharadwaj PK. Puckered-Boat Conformation Hexameric Water Clusters Stabilized in a 2D Metal− Organic Framework Structure Built from Cu (II) and 1, 2, 4, 5-Benzenetetracarboxylic Acid. Inorg Chem. 2004;43(17):5180-2.

[11] Cheng D, Khan MA, Houser RP. Copper (II) and cobalt (II) coordination polymers with bridging 1, 2, 4, 5-benzenetetracarboxylate and N-methylimidazole: coordination number-determined sheet topology. J Chem Soc, Dalton Trans. 2002(24):4555-60.

[12] Dai J-C, Wu X-T, Fu Z-Y, Cui C-P, Hu S-M, Du W-X, et al. Synthesis, structure, and fluorescence of the novel cadmium (II)− trimesate coordination polymers with different coordination architectures. Inorg Chem. 2002;41(6):1391-6.

[13] Xu Q-F, Zhou Q-X, Lu J-M, Xia X-W, Wang L-H, Zhang Y. Synthesis, structures and NLO properties of five non-centrosymmetric coordination compounds from the copper (II)/dps system (dps= 4, 4′-dipyridyl sulfide). Polyhedron. 2007;26(17):4849-59.

[14] Dobrawa R, Würthner F. Metallosupramolecular approach toward functional coordination polymers. J Polym Sci, Part A: Polym Chem. 2005;43(21):4981-95.

[15] Liu S, Yi J, Zuo W, Wang K, Wang D, Sun WH. N-(2-benzimidazolylquinolin-8-yl) benzamidate half-titanocene chlorides: Synthesis, characterization and their catalytic behavior toward ethylene polymerization. J Polym Sci, Part A: Polym Chem. 2009;47(12):3154-69.

[16] Baugh LS, Sissano JA, Kacker S, Berluche E, Stibrany RT, Schulz DN, et al. Fluorinated and ring-substituted bisbenzimidazole copper complexes for ethylene/acrylate copolymerization. J Polym Sci, Part A: Polym Chem. 2006;44(6):1817-40.

[17] Chávez-Béjar MI, Báez-Viveros JL, Martínez A, Bolívar F, Gosset G. Biotechnological production of l-tyrosine and derived compounds. Process Biochem. 2012;47(7):1017-26.

[18] Refat MS, El-Korashy SA, Ahmed AS. Preparation, structural characterization and biological evaluation of L-tyrosinate metal ion complexes. J Mol Struct. 2008;881(1-3):28-45.

[19] Zhang S, Shi W, Cheng P. The coordination chemistry of N-heterocyclic carboxylic acid: A comparison of the coordination polymers constructed by 4, 5-imidazoledicarboxylic acid and 1H-1, 2, 3-triazole-4, 5-dicarboxylic acid. Coord Chem Rev. 2017;352:108-50.

[20] Yan L, Li C, Wang Y. Syntheses, characterizations and photoluminescent properties of two novel coordination polymers constructed by poly-carboxylate and N-heterocyclic ligands. J Mol Struct. 2013;1035:455-61.

[21] Luo L, Lv G-C, Wang P, Liu Q, Chen K, Sun W-Y. pH-Dependent cobalt (ii) frameworks with mixed 3, 3′, 5, 5′-tetra (1 H-imidazol-1-yl)-1, 1′-biphenyl and 1, 3, 5-benzenetricarboxylate ligands: synthesis, structure and sorption property. Cryst Eng Comm. 2013;15(45):9537-43.

[22] Lin H, Le M, Liu D, Liu G, Wang X, Duan S. Four Cu (II)/Co (II) coordination polymers based on N, N′-di (3-pyridyl) sebacicdiamide: influence of different carboxylate ancillary ligands on structures and properties. J Coord Chem. 2016;69(6):934-46.

[23] Wang X-L, Luan J, Sui F-F, Lin H-Y, Liu G-C, Xu C. Structural diversities and fluorescent and photocatalytic properties of a series of CuII coordination polymers constructed from flexible bis-pyridyl-bis-amide ligands with different spacer lengths and different aromatic carboxylates. Cryst Grow Des. 2013;13(8):3561-76.

[24] Lin H-Y, Luan J, Wang X-L, Zhang J-W, Liu G-C, Tian A-X. Construction and properties of cobalt (II)/copper (II) coordination polymers based on N-donor ligands and polycarboxylates mixed ligands. Rsc Advances. 2014;4(107):62430-45.

[25] Boyd DB, Lipkowitz KB. Molecular mechanics: The method and its underlying philosophy. J Chem Educ. 1982;59(4):269.

[26] Cass ME, Rzepa HS, Rzepa DR, Williams CK. The use of the free, open-source program Jmol to generate an interactive web site to teach molecular symmetry. J Chem Educ. 2005;82(11):1736.

[27] Singh TB, Rey L, Gartia R. Applications of PeakFit software in thermoluminescence studies. 2011.

[28] Laugier J, Bochu B. Chekcell: Graphical powder indexing cell and space group assignment software. 2004.

[29] Montarnal D, Tournilhac F, Hidalgo M, Leibler L. Epoxy-based networks combining chemical and supramolecular hydrogen-bonding crosslinks. J Polym Sci, Part A: Polym Chem. 2010;48(5):1133-41.

[30] Sun G-M, Song Y-m, Liu Y, Tian X-z, Huang H-x, Zhu Y, et al. A novel 2D→ 3D array in a vertical mode containing both polyrotaxane and polycatenane motifs. Cryst Eng Comm. 2012;14(18):5714-6.

[31] Kuo S-W. Hydrogen-bonding in polymer blends. J Pol Res. 2008;15(6):459-86.

[32] Lu L, Jun W, Wei-Ping W, Xiu-Lan Z, Bin X. The Effect of Carboxylic Geometry on Two Cu (II) Complexes. Synth React Inorg Met-Org, Nano-Met Chem. 2014;44(3):393-6.

[33] Sun H, Tottempudi UK, Mottishaw JD, Basa PN, Putta A, Sykes AG. Strengthening π–π interactions while suppressing Csp2–H⋯ π (T-shaped) interactions via perfluoroalkylation: A crystallographic and computational study that supports the beneficial formation of 1-D π–π stacked aromatic materials. Cryst Grow Des. 2012;12(11):5655-62.

[34] Yin H, Zhao H, Zhao Y. Propylthiouracil Solubility in Aqueous Solutions of Ethylene Glycol, N, N-Dimethylformamide, N-Methyl-2-pyrrolidone, and Dimethylsulfoxide: Measurement and Thermodynamic Modeling. J Chem Eng Data. 2019;64(6):2836-42.

[35] Siesler H. Fourier transform infrared (ftir) spectroscopy in polymer research. J Mol Struct. 1980;59:15-37.

[36] Rardin RL, Tolman WB, Lippard SJ. Monodentate carboxylate complexes and the carboxylate shift: implications for polymetalloprotein structure and function. New J Chem. 1991;15(6):417-30.

[37] Bravo A, Anacona JR. Metal complexes of the flavonoid quercetin: antibacterial properties. Trans Met Chem. 2001;26(1-2):20-3.

[38] Rakha T. Transition metal chelates derived from potassium nicotinoyldithiocarbazate (KHNDC). Synth React Inorg Met-Org Chem. 2000;30(2):205-24.

[39] Kumagai H, Kepert CJ, Kurmoo M. Construction of hydrogen-bonded and coordination-bonded networks of cobalt (II) with pyromellitate: Synthesis, structures, and magnetic properties. Inorg Chem. 2002;41(13):3410-22.

[40] Chen W, Wang J-Y, Chen C, Yue Q, Yuan H-M, Chen J-S, et al. Photoluminescent metal− organic polymer constructed from trimetallic clusters and mixed carboxylates. Inorg Chem. 2003;42(4):944-6.

[41] Nakamoto K. Infrared and R aman Spectra of Inorganic and Coordination Compounds. Handbook of Vibrational Spectroscopy. 2006.

[42] Naumov P, Jovanovski G, Drew MG, Ng SW. Outer-sphere coordination, N-coordination and O-coordination of the deprotonated saccharin in copper (II) saccharinato complexes. Implications for the saccharinato carbonyl stretching frequency. Inorg Chim Acta. 2001;314(1-2):154-62.

[43] Gaber M, Ayad M, El-Sayed Y. Synthesis, spectral and thermal studies of Co (II), Ni (II) and Cu (II) complexes 1-(4, 6-dimethyl-pyrimidin-2-ylazo)-naphthalen-2-ol. Spectrochim Acta Part A: Mole Biomole Spec. 2005;62(1-3):694-702.

[44] Etaiw SEH, El-bendary MM. Structure and applications of metal–organic framework based on cyanide and 3, 5-dichloropyridine. Spectrochim Acta Part A: Mole Biomole Spec. 2013;110:304-10.

[45] Shen X-Q, Qiao H-B, Li Z-J, Zhang H-Y, Liu H-L, Yang R, et al. 3D coordination polymer of copper (II)–potassium (I): Crystal structure and thermal decomposition kinetics. Inorg Chim Acta. 2006;359(2):642-8.

[46] Gaikwad GSP, Juneja H. Synthesis, thermal degradation, and kinetic parameters studies of some coordination polymers. J Therm Anal Calorim. 2010;100(2):645-50.

[47] Ebrahimi-Kahrizsangi R, Abbasi M. Evaluation of reliability of Coats-Redfern method for kinetic analysis of non-isothermal TGA. Transac Nonferr Met Soci China. 2008;18(1):217-21.

[48] Coats AW, Redfern J. Kinetic parameters from thermogravimetric data. Nature. 1964;201(4914):68-9.

[49] Lonhienne T, Gerday C, Feller G. Psychrophilic enzymes: revisiting the thermodynamic parameters of activation may explain local flexibility. Biochim Biophy Acta (BBA) - Prot Stru Mol Enz. 2000;1543(1):1-10.

[50] Wright PV. Electrical conductivity in ionic complexes of poly (ethylene oxide). Bri Pol J. 1975;7(5):319-27.

[51] Wang H, Dlugogorski BZ, Kennedy EM. Thermal decomposition of solid oxygenated complexes formed by coal oxidation at low temperatures. Fuel. 2002;81(15):1913-23.

[52] Kandil SS, El-Hefnawy GB, Baker EA. Thermal and spectral studies of 5-(phenylazo)-2-thiohydantoin and 5-(2-hydroxyphenylazo)-2-thiohydantoin complexes of cobalt (II), nickel (II) and copper (II). Thermochim Acta. 2004;414(2):105-13.

[53] El-Sonbati A, Diab M, El-Bindary A, Mohamed G, Morgan SM. Thermal, spectroscopic studies and hydrogen bonding in supramolecular assembly of azo rhodanine complexes. Inorg Chim Acta. 2015;430:96-107.

[54] Wu C-D, Lu C-Z, Zhuang H-H, Huang J-S. Hybrid coordination polymer constructed from β-octamolybdates linked by quinoxaline and its oxidized product benzimidazole coordinated to binuclear copper (I) fragments. Inorg Chem. 2002;41(22):5636-7.

[55] Miranda M, Sasaki J. The limit of application of the Scherrer equation. Acta Crystallogr Sect A: Found Crystallogr. 2018;74(1):54-65.